We are IntechOpen, the world's leading publisher of Open Access books Built by scientists, for scientists

4,800
Open access books available

122,000
International authors and editors

135M
Downloads

Our authors are among the

154
Countries delivered to

TOP 1%
most cited scientists

12.2%
Contributors from top 500 universities

CLARIVATE ANALYTICS BOOK CITATION INDEX INDEXED

WEB OF SCIENCE™

Selection of our books indexed in the Book Citation Index in Web of Science™ Core Collection (BKCI)

Interested in publishing with us?
Contact book.department@intechopen.com

Numbers displayed above are based on latest data collected.
For more information visit www.intechopen.com

23

Carbon Nanotube Based Magnetic Tunnel Junctions (MTJs) for Spintronics Application

Elby Titus[1], Manoj Kumar Singh[1], Rahul Krishna[1], Ricardo G. Dias[2], Antonio Ferreira[2] and Jose Gracio[1]
[1]*Nanotechnology Research Division, Center for mechanical technology and automation, Department of Mechanical Engineering, University of Aveiro,*
[2]*Department of Physics and Institute for Nanostructures, Nanomodelling and Nanofabrication (I3N), University of Aveiro*
Portugal

1. Introduction

Spintronics devices exploiting the spin of the electron [1-10] are prepared to revolutionise the electronics industry. The significance of this new generation device is faster memory and lower power consumption at low electron density. The late 20th century has been considered as an era of microelectronics. However, the avalanche growth of microelectronics is a major threat to Moore's law and spintronics may be a solution for it. From the first transistor to the signally powerful microprocessor in our recent computers, most electronic devices have employed circuits that express data as binary digits, or bits (1 and 0) represented by the existence or absence of electric charge. Unlike microelectronics, spintronics exploits spin (spin up ↑ and spin down ↓) of the electron to carry information between devices.

The discovery of Giant Magnetoresistance (GMR) by Nobel Prize winners Albert Fert and Peter Grünberg had actually led to the birth of novel field spintronics [11]. Currently, most of the existing spintronic devices [12] are based on metallic systems such as magnetic tunnel junctions (MTJs) and single electron transistor [13]. On the other hand, a wealth of intriguing spin phenomena has been observed in nanoscale materials [14]. This triggered an extensive research effort on spin transport in nanoscale MTJs and other interesting phenomena were realised. One of the most important phenomena is tunnel magnetoresistance (TMR) of the MTJs. A MTJ is composed of two ferromagnetic conducting layers separated by an ultra-thin insulating layer [15-20]. The TMR was first demonstrated by M. Jullière [21]. Yakushiji et al. [22] experimentally demonstrated the influence of spin conduction on TMR. The enhancement and oscillation of TMR in ferromagnetic multiple junctions have been predicted by several authors [23-30]. However, there have been only a few experiments on spin-dependent single electron tunnelling (SET) to date [31-36] due to the difficulty in fabricating appropriate sample structures for spin-dependent SET.

The desire to build spintronic devices that show larger spin dependent phenomena has led many researchers to combine single electron tunneling (SET) and spin dependent electron tunneling (SDT). The charge quantization in low capacitance magnetic tunnel junctions

(MTJs) can lead to SET phenomena represented by Coulomb blockade (CB) below a threshold voltage and Coulomb staircase (CS) at higher voltages [37]. Carbon nanotubes (CNTs) can actually be thought of as a spacer in MTJ devices due to its one dimensional nano structure with ballistic conduction. It can control current transport by quantum mechanical spin degree of freedom. The remarkable spin dependent phenomena are expected in these devices due to the interplay between SET and spin dependent electron tunneling (SDT). In this chapter, we explore the state of the art MTJ devices with special emphasis to CNT. Novel phenomena, TMR and SET in spintronics devices are highlighted.

2. Spintronic devices

The working principle of a spintronic device follows the steps (i) information is stored into spins as an orientation (i.e. up or down), (ii) spin information is carried by mobile electrons along a path or wire and (iii) the information is then read at a final point. Figure 1 shows the schematic representation of a spintronic device. The spin orientation of conduction electrons will exist for several nanoseconds making them useful in electronic circuit and chip design. The most basic method of creating a spin-polarized current is to transport current through a ferromagnetic material and to transmit the electron spin carrying the information to the receiver point. Spin current is therefore an important tool to detect spin in spintronic devices. The important avenues for the development of spintronics devices are: (i) fabrication of nanoscale nanostructures including novel magnetic materials, thin films, hybrid structures, and functional materials, (ii) research on spin effect (spin injection, and spin transport and detection), (iii) demonstration of spintronic devices including giant magnetoresistance (GMR) and tunnel magnetoresistance (TMR) devices in magnetic tunnel junctions (MTJs) and (iv) study of SET in MTJs.

3. Magnetic Tunnel Junctions

A magnetic tunnel junction (MTJ) can be considered as a spintronic device since it is composed of two ferromagnetic materials, such as nickel, cobalt or iron, separated by an ultrathin layer of insulator with a thickness of the order of nanometre (10^{-9}m). It exhibits two resistances, low (R_p) or high (R_{ap}) depending on the relative direction of ferromagnet magnetizations, parallel (P) or antiparallel (AP), respectively. The insulating layer is so thin that electrons can tunnel through the barrier if a bias voltage is applied between the two metal electrodes. The schematic of a magnetic tunnel junction (MTJ) is illustrated in Figure 2. In MTJs the tunneling current depends on the relative orientation of magnetizations of the two ferromagnetic layers, which can be changed by an applied magnetic field. This phenomenon is called tunnel magnetoresistance (TMR). An important factor in TMR is the interaction between the electron spin (S) and angular momentum (L) that is, spin orbit coupling (SOC). An example of SOC is splitting of hydrogen spectrum [38-40]. The SOC deforms the electron shell as the direction of the magnetization rotates. This deformation also changes the amount of scattering undergone by the conduction electrons when traversing the lattice. There will be minimum resistance if the magnetizations are in parallel orientation and it will go to maximum with opposite orientations (Figure 3). Therefore, such kind of junction can be easily switched between two states of electrical resistance, one with low and one with very high resistance.

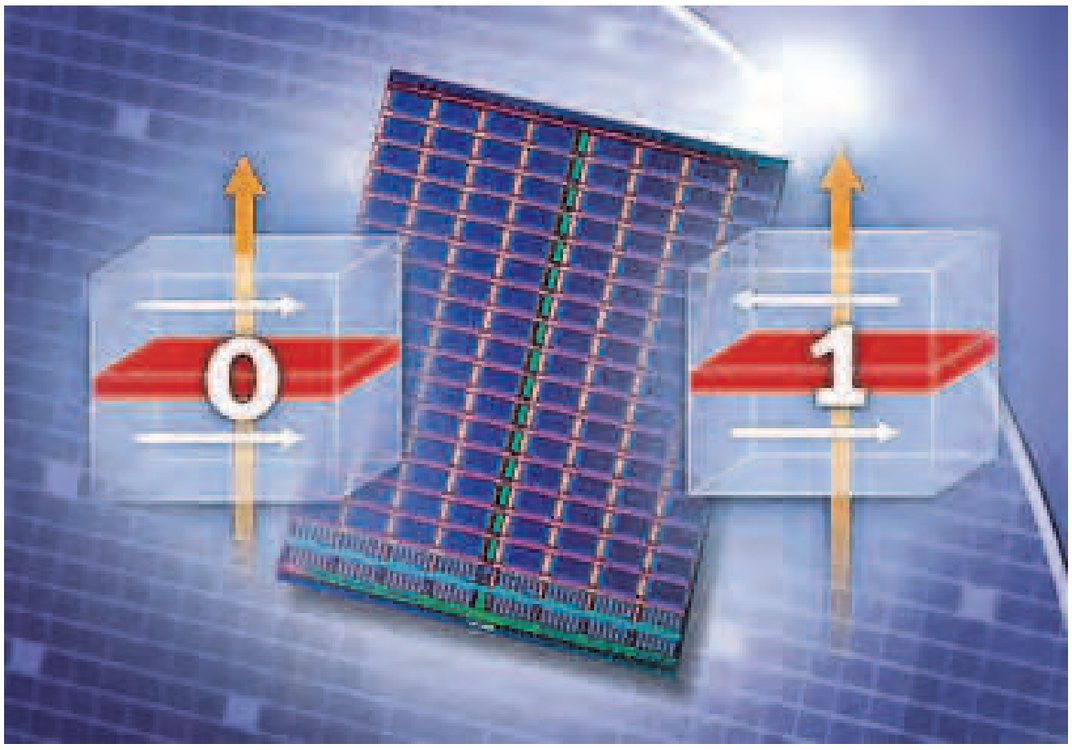

Fig. 1. A Schematic representation of spintronic device.

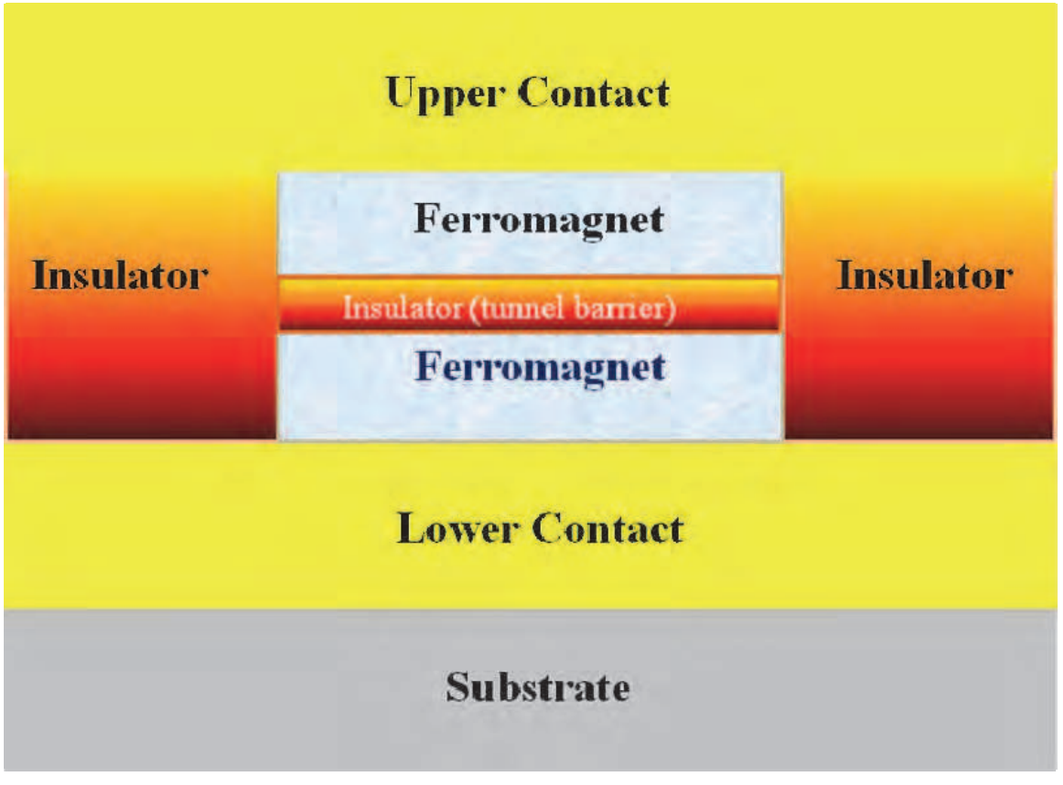

Fig. 2. A Schematic magnetic tunnel junction (MTJ).

3.1 Fabrication of MTJs

The fabrication of MTJs with high TMR ratios is crucial in developing spintronic devices. With the advance of nanotechnology, there are various methods to deposit MTJs, such as molecular beam epitaxy (MBE), magnetron sputtering, electron beam evaporation and chemical vapour deposition (CVD), and so on. In detail, the MTJ's main components are ferromagnetic (FM) layer and insulator layer. The FM layers can be fabricated by sputter deposition (magnetron sputtering and ion beam deposition). The fabrication issue is the magnetic alignment and thickness (deposition rates should be in the Angstrom-per-second range). The best way of fabricating insulating layer is still under research. Some of the proven materials are Al_2O_3 tunnel barriers made by depositing a metallic aluminium layer in the range of 5-15 Å thickness. In addition, ion beam oxidation, glow discharge, plasma, atomic-oxygen exposure and ultraviolet-stimulated oxygen exposure are also alternate ways of insulator deposition. Since the first report on TMR by Julliere [21], many studies have been performed to explore this property, especially on Al_2O_3 insulating layers. The necessity of controlling the magnetic properties of the magnetic layers introduces special requirements on the deposition process. The maintaining of inherent magnetic anisotropy is crucial in the deposition process. This can be set by applying magnetic field during deposition. The thickness & uniformity of the material, the coercivity, magnetorestriction, all are important in controlling the magnetic anisotropy.

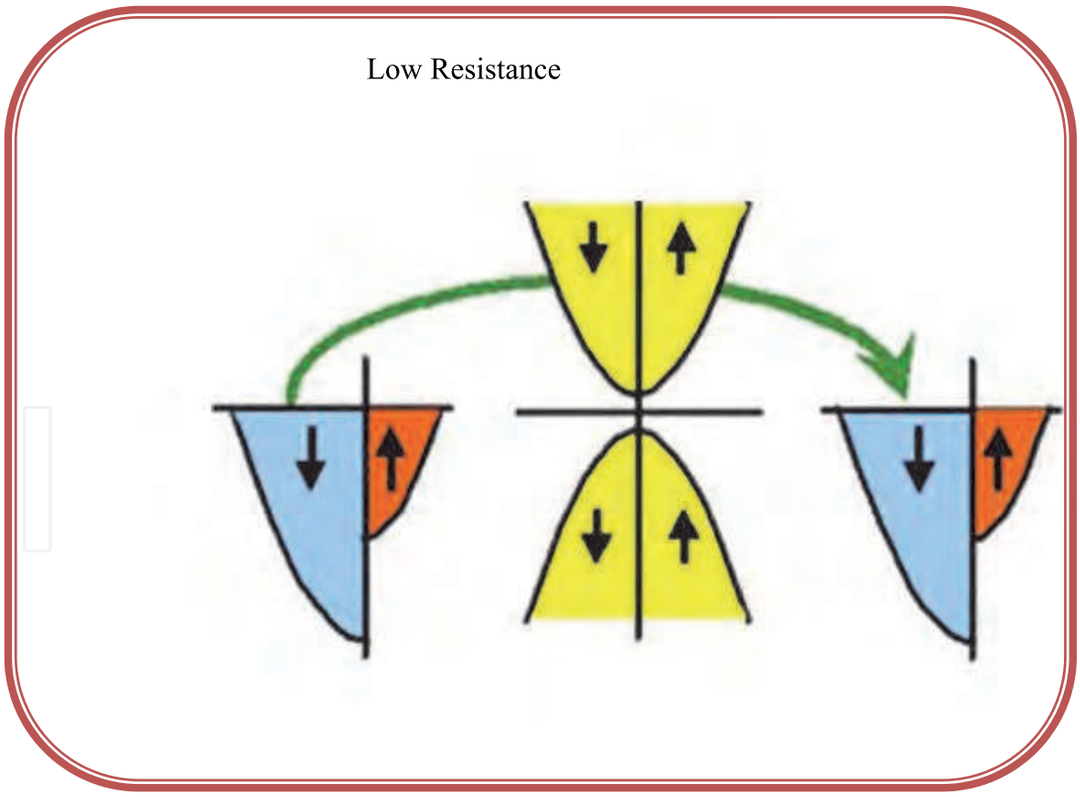

Fig. 3. Resistance goes from minimum to maximum with change in magnetization orientation from parallel to anti-parallel.

There are some theoretical predictions stating the MTJs with maximum TMR ratios could be fabricated by the epitaxial growth of ferromagnetic-non ferromagnetic-ferromagnetic nanoscale sandwich structure, Fe/MgO/Fe and Fe/MgO/FeCo [41, 42]. The high ratios resulted from the effective coupling of the majority spin band of Fe/FeCo into MgO and MgO into Fe/FeCo. TMR ratios up to 180% and 220% were achieved in these structures [43, 44]. The literature also says MTJs can be fabricated using half-metallic ferromagnets [45] and can generate 100% spin polarization at Fermi level (EF) due to the energy gap for one spin direction. The maximum spin polarization up to 100% is highly desirable in spintronic devices for the efficient spin injection from ferromagnetic electrodes into the non-ferromagnetic spacer and for the development of current induced magnetization switching in MTJs. Other MTJs with half-metallic ferromagnets which have shown higher TMR at room temperature are cobalt based alloy thin films including $Co_2Cr_{1-x}Fe_xAl$, Co_2MnSi or Co-Mn-Al. In addition to MgO tunnel barrier, aluminium oxide also been used as tunnel barrier with ferromagnetic electrodes $Co_2Cr_{0.6}$ $Fe_{0.4}$ Al and Co_2MnSi. The advantage of these alloys is the high Curie temperature above room temperature. N. Tezuka et al have developed a MTJ of $Co_2FeAl_{0.5}Si_{0.5}$ electrodes and a MgO barrier fabricated by MBE and observed that their device had a TMR ratio of 386% at approximately 300K and 832% at 9K [46]. Nowadays, magnetic data storage technologies prefer perpendicular magnetic anisotropy (PMA) compared to the conventional devices that exploit the magnetization of the layers within the film plane. Figure 4 shows the cell structure with perpendicular magnetic anisotropy. An alloy of cobalt-iron is employed in the magnetic layer, with magnesium oxide in the insulating layer and cobalt-iron-boron in the interface layers. The structure developed by Toshiba is used for recording media. PMA has also been observed in several ferromagnetic materials including multilayers such as Co-Pt, Co-Pd, Co-Ni, CoFe-Pt, and CoFe-Pd, Co-Cr-Pt, alloys such as CoPt, FePt, and CoCr, and rare-earth transition metal alloys [47-50]. However, an ideal system with high thermal stability at nanoscale dimension, low current induced magnetization and high TMR was not successful. In view of this, S.

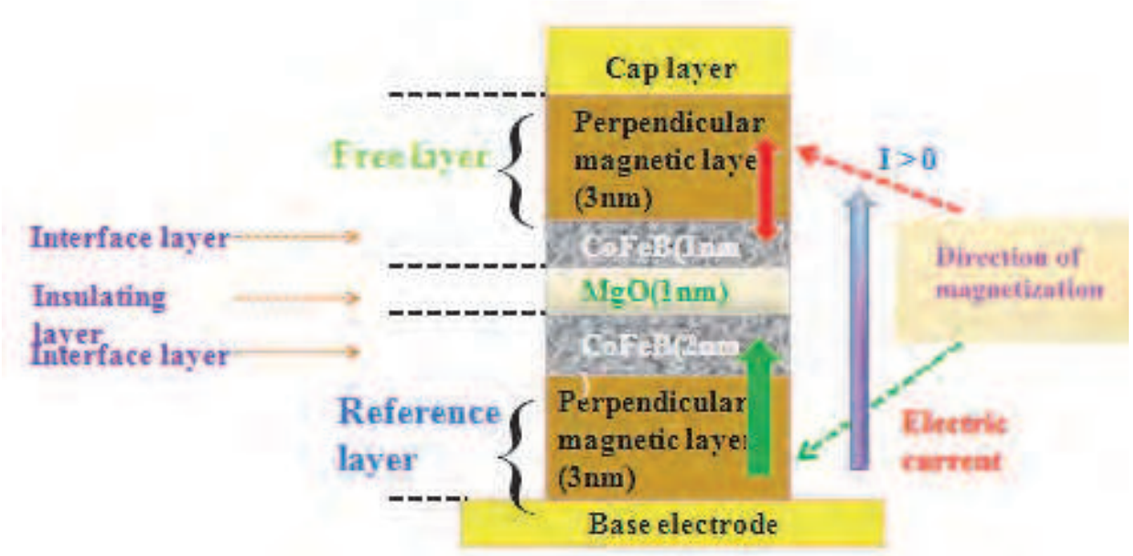

Fig. 4. Magnetoresistive random access memory (MRAM) with giga bits capacity developed by Toshiba.

Ikeda et al [51] employed interfacial PMA between the ferromagnetic electrodes and the tunnel barrier of the MTJ by using the material combination of CoFeB–MgO. The MTJs consisting of Ta/CoFeB/MgO/CoFeB/Ta showed a high TMR ratio, over 120%, high thermal stability at dimension as low as 40 nm diameter and a low switching current of 49 μA.

3.2 TMR in MTJs

To continue the discussion, TMR is a magnetoresistive effect that occurs in component consisting of two ferromagnets separated by a thin insulator (MTJ). The interest towards TMR is driven by the fact that MTJs with spin dependent tunneling (SDT) are expected to provide technical promises that will allow the realization of nanoscale devices in more advanced spintronic applications. T. Moodera et al [52] fabricated the first reproducible TMR up to 24% (Figure 5) at room temperature on CoFe/Al_2O_3/Co or NiFe junction. Today, reproducible TMR value up to 50% can be obtained with three dimensional ferromagnets making them useful for industrial application [53].

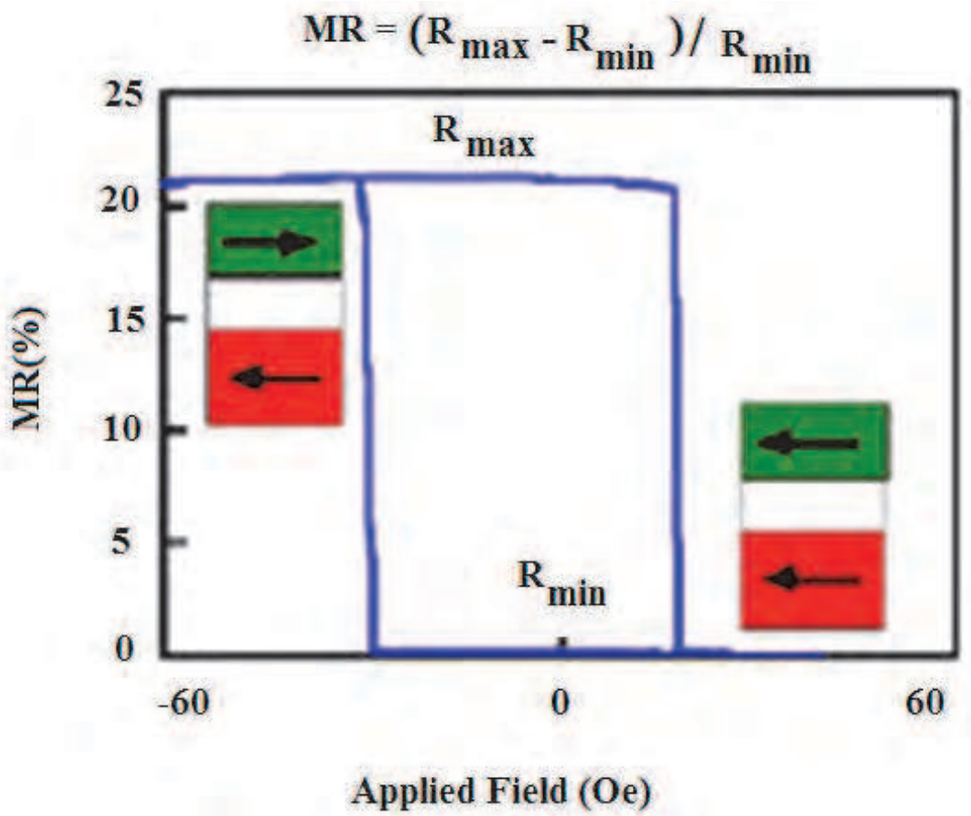

Fig. 5. Ratio of tunnel magnetoresistance (TMR) shown in CoFe/ Al_2O/ Co junction., J. S. Moodera, L. R. Kinder, T. M. Wong, and R. Meservey, Phys. Rev. Lett. 74, 3273 **(1995)** © American Physical Society

3.2.1 Theory of TMR

The TMR effect in MTJs can be derived using Julliere's model [21, 51-53]. According to this model the magnetoresistance,

$$\text{TMR} = (R_{AP}-R_P)/R_P = 2P^2/(1-P^2) \quad (1)$$

where R_P *and* R_{AP} are the resistance in parallel and antiparallel magnetic configuration, respectively and P is the spin polarization. The Differential TMR can be re-written as

$$\text{TMR} = \frac{\left(dI/dV_{AP}\right)^{-1} - \left(dI/dV_P\right)^{-1}}{\left(dI/dV_{AP}\right)^{-1}} \quad (2)$$

According to Wiesendanger [54] the derivative of an *I-V* curve (the differential conductivity is expressed as

$$\frac{dI}{dV} = \left(\frac{2\pi e^2}{\hbar}\right) |t|^2 D_1(E_F) D_2(E_F + eV) \quad (3)$$

where $|t^2|$ is the tunnel probability, D_1 and D_2 are the DOS of the two electrodes, E_F is the Fermi energy, and V is the bias voltage applied to the electrode at low temperature.

The injection of spin currents from a ferromagnetic manganite, $La_{0.7}Sr_{0.3}MnO_3$, into a single CNT (non-ferromagnetic) and the transformation of spin information into large electrical signal have been demonstrated by L. E. Hueso *et al* [55]. The TMR calculated in their system is 61%. R. S. Liu *et al.* [56] observed TMR (10%) due to the interplay of SDT and CB in a Ni/NiO/Co/NiO/Ni double junction of a submicron scale. Interestingly, both the systems are MTJ which is similar to our system. H.B Peng et al. [57] also studied I-V characteristics on patterned growth of SWCNT arrays from vapour-deposited Fe catalyst. Similar I-V features were observed in Nickel-CNT-Nickel MTJ system fabricated by the current authors [58]. Undoubtedly, Coulomb blockade (CB) effect, the principle of single electron tunnelling (SET), is responsible for the enhanced TMR in nanoscale MTJs. The SET phenomena and the associated MR occur only if the transport of electrons from one electrode to another is inhibited due to the extremely high electrostatic energy $e^2/2C$ (e = charge of electron and C is the capacitance) of a single electron compared to the thermal energy k_BT. When the bias voltage increases and exceeds the threshold $V^{th} = e/2C$, the current starts to increase. If the resistance of two junctions are similar (R1≈ R2), the current increases smoothly with bias voltage. T. Niizeki et al [59] could reduce the junction area to 10nm and observed enhanced TMR due to the coulomb blockade (CB) effect.

Motivated by the possibility of spintronics, the current authors have attempted a novel MTJ system using vertically aligned CNTs [58, 60]. The TMR along with Coulomb blockade and Coulomb staircase was observed in our system. Our device is formed of a vertical array of carbon nanotubes bridged between the nickel electrodes. The higher value of CB spacing (~ 2 V) in our system compared to the reported value (0.8V) is expected due to the bulk effect of CNT arrays. It also confirms that there is no short connection in the sample. From the I-V analysis of our system it appears that TMR is originating from the spin polarisation of the electrodes, i.e the difference between the density of states (DOS) of the up-and down-spin sub-bands in the two electrodes. More details of CNT- MTJs are given section 2.2.

3.2.2 Characterization

It is well known that the TMR is highly sensitive to the structural and chemical nature of the material. The characterization techniques such as electrical conductivity, magnetoresistance

and tunneling microscopy can give detailed information on MTJs properties. The knowledge on magnetic property of the ferromagnetic electrodes is crucial in development of MTJ devices. The superconducting quantum interference device (SQUID) is the most sensitive magnetic field equipment to measure the magnetic property. It has enough sensitivity to measure measure the magnetic fields in nanoscale ferromagnets. The magnetization of the material can also be measured by vibrating-sample magnetometer (VSM) technique. VSM is based on Faraday's law which implies that an emf will be generated in a coil when flux changes in the coil. TMR also can be measured using the four probe method by sweeping the magnetic field. Scanning tunneling spectroscopy (STS)/scanning tunneling microscopy (STM) is another technique which can give precise TMR measurements. The details of all these measurements are given in section 5.

3.3 Application of MTJs

With wider knowledge on how to manipulate spins [61], we can build more state of the art spintronic devices with extraordinary properties. Extended research into application possibilities of any spintronic effects is therefore crucial to realise more advanced spintronic devices. These devices made huge impact on computer technology by enabling higher storage of information in hard drives and faster reading of data in random access memories. The first successful application of MTJ was demonstrated in computer read head technology with Al_2O_3 barrier and MgO barrier MTJ. The magnetic recording density in hard disk drive increased (300-600 Gbit/Inch^2) considerably in these devices [62-65]. Another application of MTJ is to develop magnetic random access memory (MRAM) devices. It has been claimed that MRAM can exceed the speed of SRAM (static RAM), density of DRAM (Dynamic RAM) and non-volatility of flash memory. In addition, the nano-dimension device has low power consumption and less heating. MRAM is an upgrade version of SRAM and DRAM where data is stored using spin instead of electrical charges. It overcomes one of the disadvantages of the conventional RAM, the loss of information by power failure. Leading companies like IBM, Motorola, and Honeywell started the MRAM research in 1995 and they were supported by United States Defense Advanced Research Projects Agency (DARPA). Figure 6 shows the images of MRAM used by leading companies like Thoshiba, IBM and Motorola.

4. Spin current in MTJs

In the view of rapid progress in the fabrication of nanoscale MTJs, spin is a subject of great interest. Spin is a purely quantum mechanical quantity which provides an extra degree of freedom for the electron to interact with a magnetic field. In 1922, Stern and Gerlach demonstrated the most direct experimental evidence of the existence and of the quantized nature of the electron spin. The first experimental evidence of spin dependent tunneling was reported by Jullerie [21] in 1975. Later, Berger proposed the idea that spin polarized current act on local magnetization of ferromagnets and leads to giant magnetoresistance [66]. The important property of spin is its weak interaction with the environment and with other spins, resulting in a long coherence or relaxation time, which is a very important parameter in the field of spin-transport and quantum computing. For the successful incorporation of spins into the currently existing electronics, one has to resolve issues such as efficient spin injection, spin transport, control and manipulation of spins and finally detection of spin polarized current.

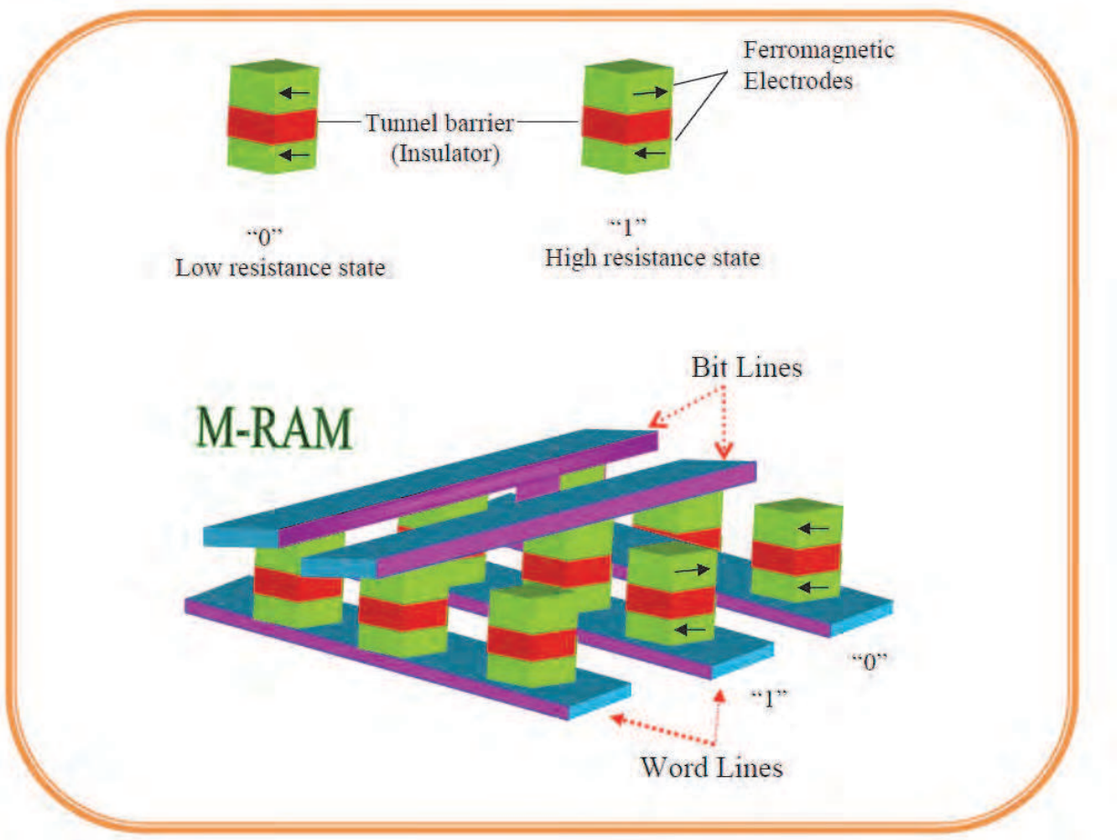

Fig. 6. MRAM memory cells composed of a magnetic tunnel junction (MTJ). States "0" and "1" in the cells correspond to the parallel and antiparallel alignments of the electrode magnetic moments.

Spintronics without magnetism is an attractive pathway for designing semiconductor spintronic devices since spin orbit coupling (SOC) enables that the spin is generated and manipulated merely by electric field. By the application of electric field, the electrons move in the lattice generating a magnetic field which acts up on the spin. The spin orbit interaction on mobile electrons was proved theoretically many decades ago. However, the practical harnessing of this concept is still at an early stage

4.1 Spin transport

The influence of spin transfer in MTJs can be observed by measuring resistive loops as a measure of external applied field and applied voltage. By sweeping the magnetic and electrical field, one can observe sharp drop in resistance which is attributed to the switching from parallel to antiparallel and vice versa. The drop of resistance is associated with the TMR. One of the factors that affect drop of resistance and TMR is density of states (DOS) at the interface [67-71].

4.2 Spin polarization

In addition to the spin transport, spin injection and spin polarization also an important factors in governing TMR. The spin polarization is a result of a subtle cancellation between

two spin channels and is greatly influenced by the atomic, electronic and magnetic structures of the system. While the fundamentals of electron tunnelling are well understood, the quantitative theoretical description is lacking in real systems due to limitations in fabrication. Sophisticated and stable nanofabrication method will solve the problem of interface in MTJs. However, to build up on experimental findings, it is also essential to develop an accurate model of the spin polarization and transport of spin current through the ferromagnetic/nonferromagnetic interface and finally into vacuum which is highly sensitive to the chemical and material details of the device. In this context, Density functional theories [72] of MTJ system that can produce spin polarization effects in the Fermi Energy (FE) are important. Density functional theory (DFT) is a widely used method for modelling charge/spin carrier transport semiconductors. There is plenty of literature on DFT based calculations in studying SDT in MTJs [73-75]. The key components in the modelling are schottky barrier (φ_b) and the applied voltage V_A against current density. Ab initio simulation of magnetic tunnel junctions has been demonstrated by Derek Waldron *et al* [76]. The effect of schottky barrier profile on spin dependent tunnelling in a ferromagnet-insulator-semiconductor system is reported in N.L.Chung *et al*'s work [77].

4.3 Theoretical modelling

Landauer [78] formula is really useful in order to compute spintronic devices. For the simplicity of modelling, the system can be assumed as one-dimensional, composed by a quantum wire with length L and two ferromagnetic reservoirs with electrochemical potential μL and μR which are given by

$\mu L^{\uparrow\downarrow} = E_F + (-)\Delta\mu$,

$\mu R^{\uparrow\downarrow} = E_F + (-)\Delta\mu + V_A$,

$\Delta\mu = (\mu\uparrow - \mu\downarrow)/2$ being half of the spin splitting energy. The effect of the Schottky barrier is important on the SDT and therefore negligible spin relaxation in the tunnel barrier should be considered.

If *f* is a function in the k space, the sum of f over k is given by

$$I = \sum_{\mathbf{k}} f(\mathbf{k}) \tag{4}$$

Let us assume that the transport in the channel is ballistic and the electrons entering the reservoir is in equilibrium. The positive current, carried by the k> 0 state in i subband is then given by

$$I_i^{>} = \frac{q}{L} \sum_{k>0} v_i(k) f(E - \mu_L) \tag{5}$$

where υi is the velocity and f is the Fermi-Dirac distribution function.

Using

$$\sum_k f(k) \rightarrow 2\,\frac{L}{2\pi} \int f(k)dk \tag{6}$$

eqn 6 can be rewritten as

$$I_i^{>} = \frac{q}{\pi}\int_0^{\infty} v_i(k) f(E-\mu_L)dk \tag{7}$$

Since $v_i = \frac{2\pi}{h}\frac{\partial E}{\partial k}$, the positive current can be expressed as

$$I_i^{>} = \frac{2q}{h}\int_{\epsilon_i}^{\infty} f(E-\mu_L)dE \tag{8}$$

where h is the Planck's constant and ϵ_i is the cutoff energy of the i subband. The negative current is similarly given by

$$I_i^{<} = \frac{2q}{h}\int_{\epsilon_i}^{\infty} f(E-\mu_R)dE \tag{9}$$

and the total current as

$$I = I^{>} - I^{<} = \frac{2q^2}{h} M \frac{\mu_L - \mu_R}{q} \tag{10}$$

$$M(E) = \sum_i u(E-\epsilon_i), \tag{11}$$

is the number of modes in subband i having energy less than E, and u is a Heaviside function. Low temperature has been assumed so that $f(\epsilon-\mu) \approx u(\mu-\epsilon)$ and M has been assumed to be constant in the energy range

$$\mu_2 < \epsilon < \mu_1 . \tag{12}$$

The total current density will be calculated by adding current of each spin channel,

$$I = I\uparrow + I\downarrow \tag{13}$$

and the spin current is given by the difference between up spin and down spin currents.
The introduction of a 3D system can further increase the consistency of calculation compared to 1D.
In this review, we emphasis on graphene and CNTs based MTJs which are the most recent attractions in MTJ research.

5. Graphene based MTJs

Graphene is the building block of graphite and it is made from a hexagonal lattice of carbon atoms with sp^2 bonds (Figure 7). Graphene is a promising material for spintronics and MTJs due to its intrinsic spin orbit interaction [79-87]. The electron spin of graphene also has interaction with the carbon nuclei. In addition, its unique properties, especially long spin flip length up to 1μm at room temperature enhances its potential to spintronics. They also show half integer quantum hall effect and high electrical conductivity. Many groups have studied TMR for graphene connected to ferromagnetic leads. They have demonstrated injection of spin polarized current in the system. Graphene is ideal for application of spin

valve effect in which the resistance of the devices can be changed by manipulating the relative orientation of the magnetization. Hill et al [88] fabricated a spin valve device consisting of a graphene connected by two FM leads and investigated a 10% change in resistance as the electrodes switch from parallel to antiparallel state.

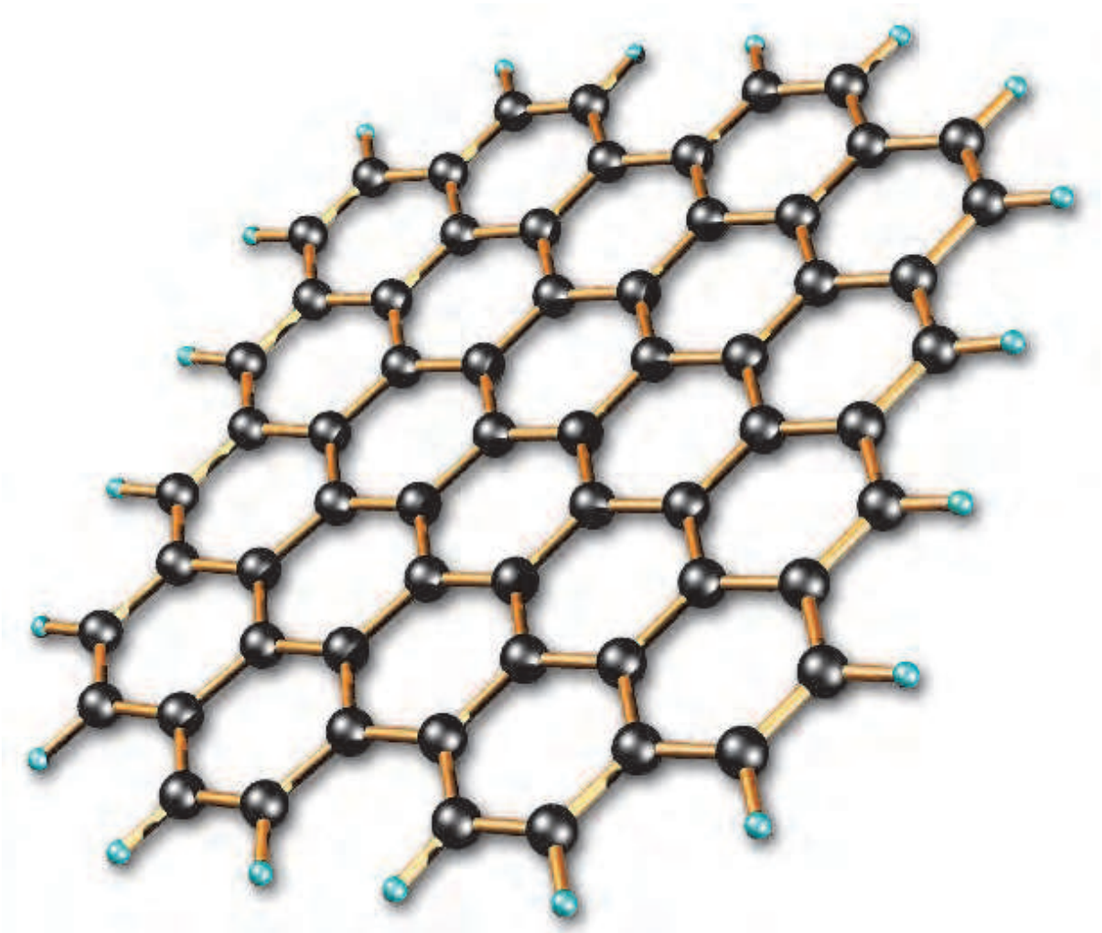

Fig. 7. Graphene showing the 2-D network of sp^2 bonded carbon atoms.

Experimentally, there have been few evidences for spin-polarized transport in graphene spin valves [89]. Wang et al investigated the magnetoresistance (MR) properties of quasi-two-dimensional mesoscopic graphite (MG) spin valve devices consisting of flakes with thickness between 1 and 40 nm (3 to 100 layers of graphene) contacted by two ferromagnetic electrodes and observed signatures of spin-polarized transport for MG flakes in the thickness range 10–40 nm. For devices in which an ultrathin magnesium oxide (MgO) tunnel barrier is inserted at the FM/MG interface, the spin valve effect has been observed with MR magnitudes up to 12% at 7 K and signals persisting up to temperatures as high as 60 K. In contrast, the spin valve effect has not been seen in devices without MgO, suggesting the importance of spin-dependent interfacial resistance for spin injection into MG [90-92]. Investigation of the voltage bias dependence of the MR finds a reduction of the MR with increasing voltage and a correlation with the differential conductance. Finally, the spin valve signal exhibits oscillatory MR as a function of gate voltage [93-95].

6. Carbon nanotubes based MTJs

Carbon nanotubes (CNTs) [96] are molecular tubes of carbon with outstanding properties (Figure 8). They are among the stiffest and strongest materials known, and have remarkable electronic behaviour and many other unique properties. They are attractive for spintronic devices due to their nanoscale size, extremely large spin flip scattering lengths and because they can behave as one-dimensional ballistic quantum conductors [97-102]. Experimental investigations on coherent spin transport through Co-contacted CNTs showed that spin can be coherently transported over 130 nm through the carbon nanotube [103].

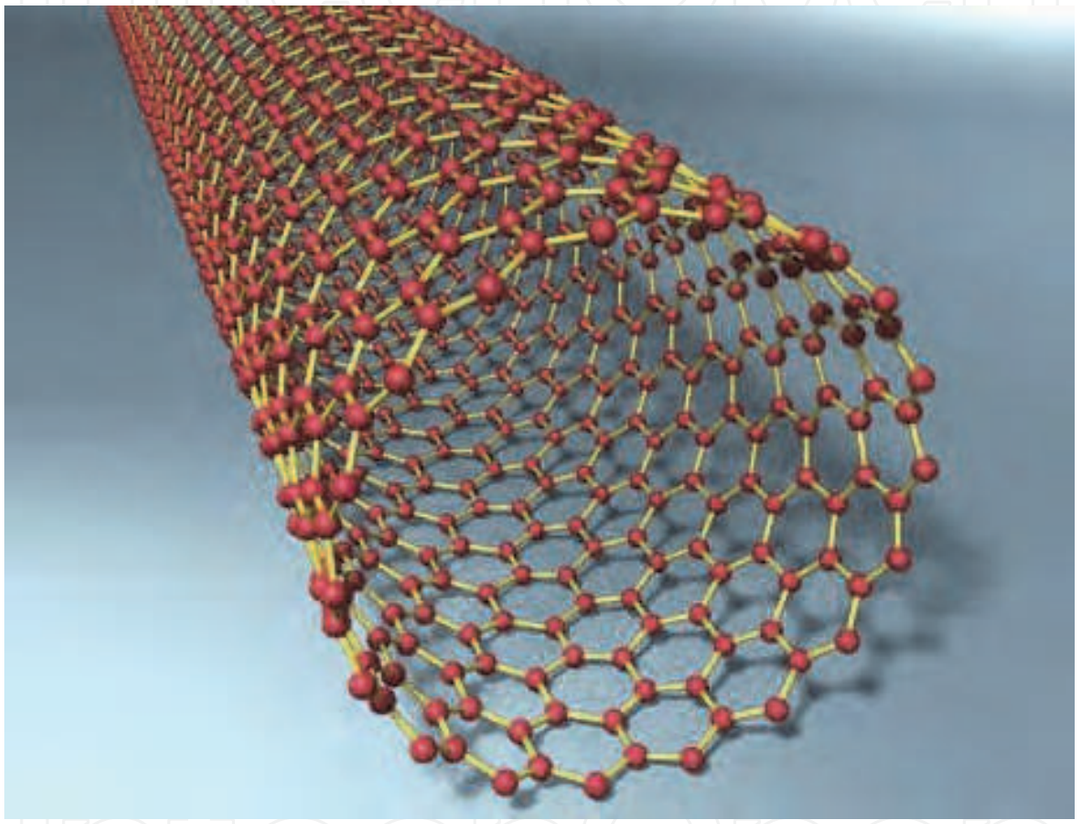

Fig. 8. Image of a carbon nanotube.

6.1 Fabrication of vertically aligned carbon nanotubes

Various conventional methods have been used to grow CNTs, including arc-discharge, laser ablation, and chemical vapor deposition (CVD). However, only chemical vapour deposition (CVD) methods allow the controlled growth directly on a substrate, which is important for many applications, especially as the individual manipulation of CNTs is difficult and expensive, due to their reduced size. The orientation of CNTs is highly important in achieving the maximum benefit of its property. The ability to pattern or position carbon nanotubes (CNTs) with a vertical orientation in controlled arrays has been demonstrated by many researchers [104-106]. Conventional plasma enhanced (PE) CVD is an established technique for the synthesis of vertically aligned CNTs[107-110]. Selective, aligned growth of CNTs on silicon and glass substrates has been demonstrated by plasma enhanced chemical

vapor deposition. However, despite the high level of control, PECVD growth typically involves processing temperatures over 900 ^{o}C, which significantly limits the choice of the possible substrate materials and the integration processes. Bonard et al[6] have demonstrated in their work that the enhanced field emission factors of individual CNTs (30 000-50 000) are very large, when compared to the CNT films (1000-3000) [111-112]. The smaller field emission factors in the CNT film have been considered a consequence of the effect of the planar substrate supporting the CNT film. The field-enhancement factors of dense CNT films were even smaller because the electric field on one tube is screened by the proximity of neighboring tubes.

We reported the selective growth of VACNTs on large area copper substrates using a double plasma hot-filament chemical vapour deposition system (DP-HFCVD) [JNN paper 113]. We employed our modified HF-CVD system (Figure 9) for the deposition of large area (1-1.5 inch^2) carbon nanotubes onto nickel electroplated copper substrates. The system employed three independent power supplies, which were used to generate two independent plasma glow discharges within the vacuum chamber. The system consisted of two parallel molybdenum plates sandwiching a resistive tantalum filament. Each of the two molybdenum plates was electrically biased, either positively or negatively, with respect to the filament, in order to generate the two glow discharges. The precursor gases used were methane and hydrogen (gas flow: 46/200 sccm) at 7 mbar. The DC voltage (0-600 V) was applied between the upper substrate electrode and the filament. The filament power was maintained at 600 W and the substrate temperature (650 ^{o}C) was measured using a sealed thermocouple placed inside the substrate holder immediately beneath the substrate.

The growth of the CNTs involves three processes: (i) substrate pretreatment, (ii) nucleation and (iii) the actual growth of the CNTs.

(i) A 0.8 mm thick flat copper substrate with 98% purity was treated by sand blasting and then cleaned in ultrasonic acetone bath. The cleaned substrate was subsequently electroplated with nickel in a nickel sulphate bath. The copper substrates were used as the cathode and a nickel rod served as the anode. The 50 nm nickel coated copper substrates were subsequently transferred to the HF-CVD chamber and the chamber was purged by 100 sccm hydrogen gas for a few hours.

(ii) For the nucleation, the substrates were exposed to hydrogen plasma, promoting the etching of the catalyst and enabling the formation of nickel nano-clusters.

(iii) Finally, the CNTs were grown with hot filament power in the presence of precursor gases, methane and hydrogen.

The morphology of the CNTs deposited at different times was examined using SEM microscopy. Figure 10 shows the SEM image of CNTs deposited by DP-HFCVD (a) and conventional CVD (microwave) (b) in 2 hours. Unlike the conventional CVD CNTs, the DP-HFCVD CNTs appeared highly dense and were grown perpendicular to the substrate. It is reported that the growth rate in plasma enhanced (PE)CVD is generally slower than that in thermal CVD, which may be partly due to the atmospheric pressure operation of thermal CVD [114]. The CNTs grown by DP- HFCVD system also showed a slow growth rate and, taking almost 2 hours to form a forest of tubes. Bower *et al* [115] showed the effect of the electric field on the alignment of nanotubes unambiguously in a microwave plasma of acetylene and ammonia. Initially, when the plasma was on, their multiwalled (MW) CNTs were vertical; when growth proceeded with plasma off (in a thermal CVD mode), the nanotubes were found to be curly or randomly oriented. They also found that nanotubes

always grew perpendicular to the substrate surface regardless of the substrate position or orientation. Since their work, a number of articles have appeared, considering the general orientation of PECVD-grown nanotubes better than the results from thermal CVD [116]. However, all these works were concentrated only on vertical alignment of the tubes, and the adherent properties of the tubes were ignored.

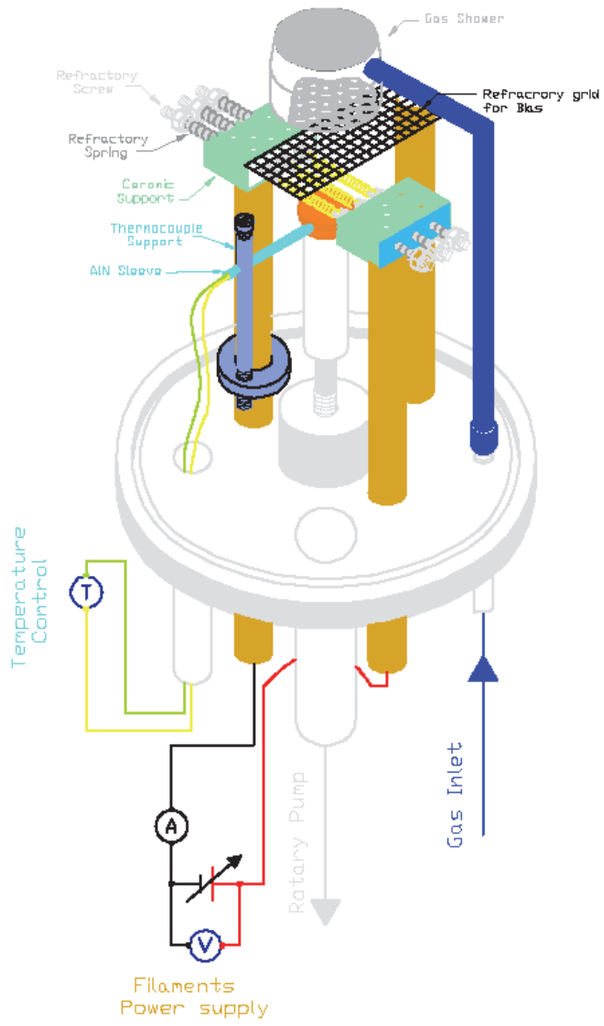

Fig. 9. Computer drawing of DP- HFCVD system.

The quality of the CNT was confirmed by Raman Spectroscopy. Figure 11 shows the micro-Raman spectra for samples (a) VACNT and (b) conventional CVD. The most prominent features in the first-order Raman spectra were observed for both the samples positioned at around 1570cm^{-1} (G band) and 1350cm^{-1} (D band). The peaks positioned at 1350 cm^{-1} represent the disorder-induced phonon mode (D-band) and the strong peak at 1577 cm^{-1} (G-band) can be assigned to the Raman-allowed C-C phonon mode (E2g-band) [117]. A small difference in the D and G peak positioning was noted with these samples and we attribute this to the structural differences in the tubes.

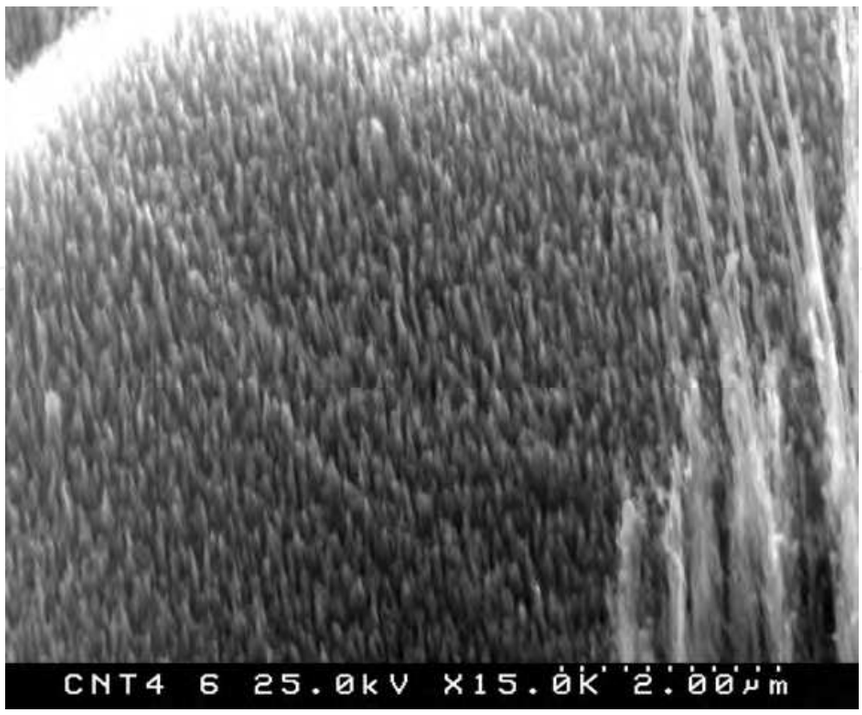

(a)

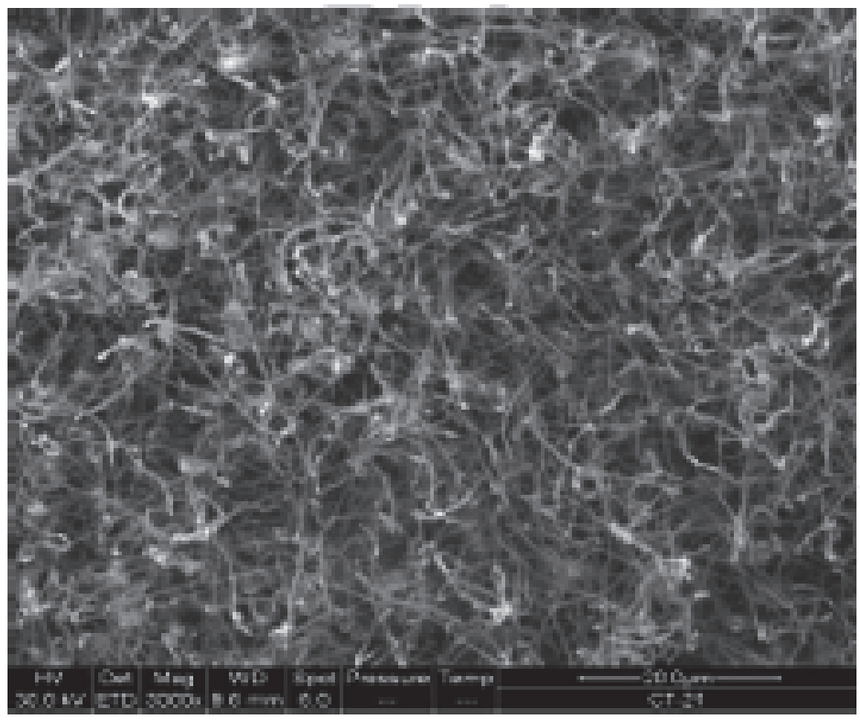

(b)

Fig. 10. SEM images of CNTs deposited by (a) DP-HFCVD and (b) Conventional CVD (micro-wave) in 2 hours.

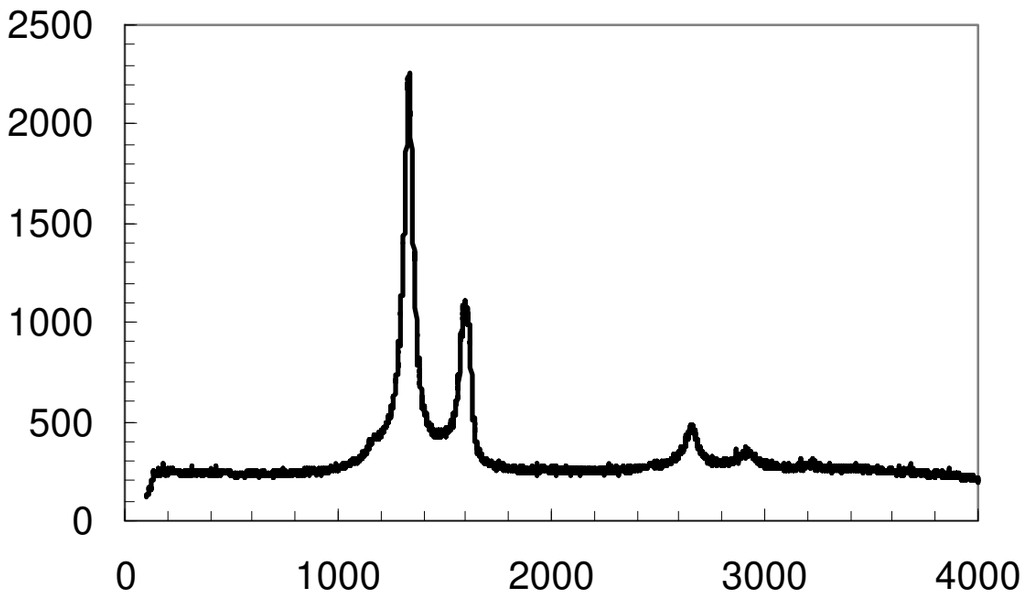

Fig. 11. Micro-Raman spectra of VACNT.

6.2 TMR in CNT based spintronic devices

Since its discovery, a large number of nanodevices such as single electron transistor, Light emitting diode, field effect transistor has been demonstrated. However, these devices are based on charge of the electron. TMR characteristics have already been measured in CNTs both experimentally and theoretically [118]. K Tsukagoshi et al [103] demonstrated the MR in a single CNT contacted by ferromagnetic metal electrodes. The spintronic devices exhibiting TMR using ferromagnet-contacted single walled carbon nanotubes (SWCNTs) have been demonstrated by A. Jensen *et al* [118]. Most of the reports on CNT-TMR system are mainly based on single carbon nanotube contacted to bulk ferromagnetic material by an *ex-situ* method [119-121]. The TMR effect is also known to be sensitive to the tunnel barrier/electrode interface. The barrier sensitivity may be more evident in a system with single CNT. De Teresa *et al* [122] studied ferromagnetic MTJ with various barrier materials and found that even the sign of the TMR depends on the barrier materials. S. Yuasa *et al* [123] also investigated the effect of crystal anisotropy of the spin polarisation on MTJ using single crystal iron electrodes of various crystal orientations. They found a clear crystal orientation dependence of the TMR which might reflect the crystal anisotropy of the electronic states in the electrodes.

The current authors followed a different approach for the development of a potential MTJ device. The details are discussed below.

Figure 12 shows the Field-Emission Scanning Electron Microscopy (FE-SEM) image of the MTJ system fabricated by the current authors. The Ni nanoparticles (on top, ~1μm in thickness) deposited on top of the VCNTs are apparent in figure 12. High density well aligned MWCNTs with length larger than 2 μm are apparent in the image. The details of the substrate pre-treatment method, the formation of nanoclusters and the synthesis of

vertically aligned MWCNTs on nickel plated copper substrate using a double plasma method is reported in our previous paper [124]. Energy Dispersive X-ray microanalysis (EDS) attached to the FE-SEM reveals Ni nanoparticle deposition on the top surface of VCNTs. The magnified FE-SEM images of the green dashed square areas marked by 1 and 2 in Figure 12 are illustrated in inset. Unlike CNTs grown by conventional techniques, VCNTs grown by DP-HFCVD technique are short (~ 2μm), isolated and vertically aligned to the substrate. The green dotted square area 1 illustrates the VCNTs covered by nano nickel paticle. However, the particles are less in the lower portion of the sample (Green dashed square area 2).

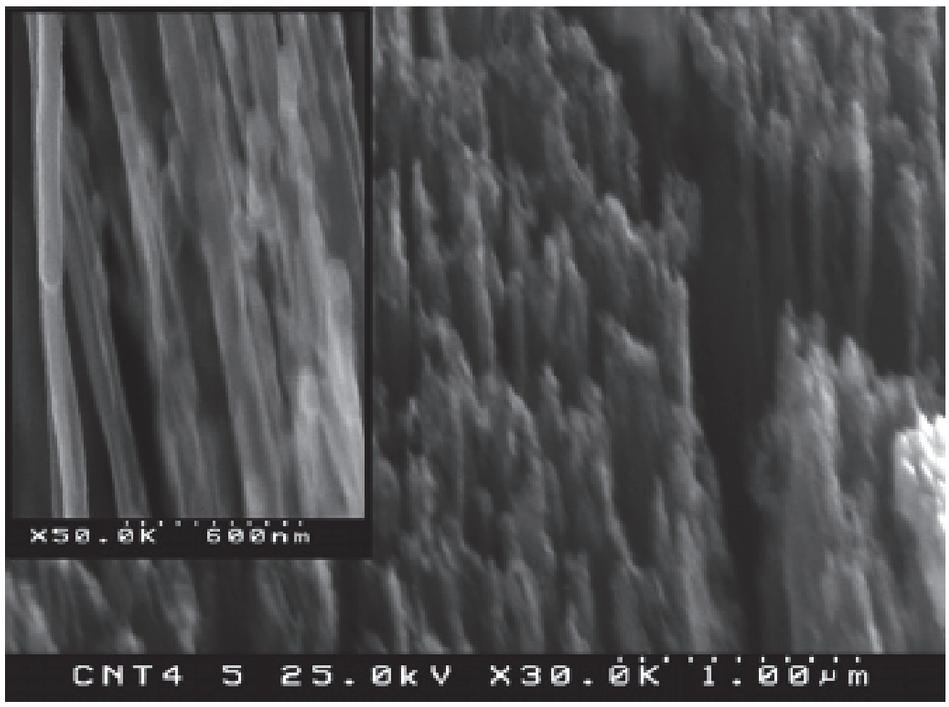

Fig. 12. FE-SEM image of the VCNT sample deposited with nickel nanoparticles. The inset shows a magnified FE-SEM image displaying isolated VCNTs.

TMR/GMR is known to originate from spin interaction between the magnetic and nonmagnetic particle at the interface and are related to the coercivity value [125]. To probe the magnetic properties, the field dependence of the magnetization was measured using a superconducting quantum interface device (SQUID) [126]. Figure 13a shows magnetization *vs.* applied magnetic field for nickel nanoparticle deposited VCNTs at 2 K and 300 K, respectively. It indicates that the sample exhibits ferromagnetic behaviour with a hysteresis loop at 2 K and 300 K, respectively. The saturation magnetization (M_s), coercivity (H_c), and remnant magnetization (M_r) for both temperatures are summarized in Table 1. The saturation magnetization values and coercivity for nickel nanoparticle deposited VCNTs shows a decrease from 5.3 to 4.4 emu g^{-1} and 395 to 115 Oe, respectively, with the increase of temperature, indicating a characteristic ferromagnetic behaviour. To gain a better understanding of the magnetic behaviour of nickel nanoparticle deposited VCNTs, we have performed zero-field-cooled (ZFC) and field cooled (FC) magnetization measurements. For

the ZFC measurement, the nickel nanoparticle deposited VCNTs sample is first cooled from 300 to 2 K in zero magnetic field. On the other hand, for FC measurements, the sample is cooled in the magnetic field (25 Gauss) from 300 to 2 K, and later the magnetization is measured in the warming cycle keeping the field on. Figure 13b shows the temperature dependence of ZFC and FC measurements under the applied magnetic field of 25 Gauss for nickel nanoparticle deposited VCNTs which exhibits the main features of ferromagnetic behaviour [127]. The blocking temperature T_B (transition temperature from ferromagnetic to superparamagnetic state) peak can be observed in ZFC curve at about ~44 K. The low value of T_B is directly in agreement with smaller size of nickel nanoparticles randomly deposited on the VCNTs [128,129].

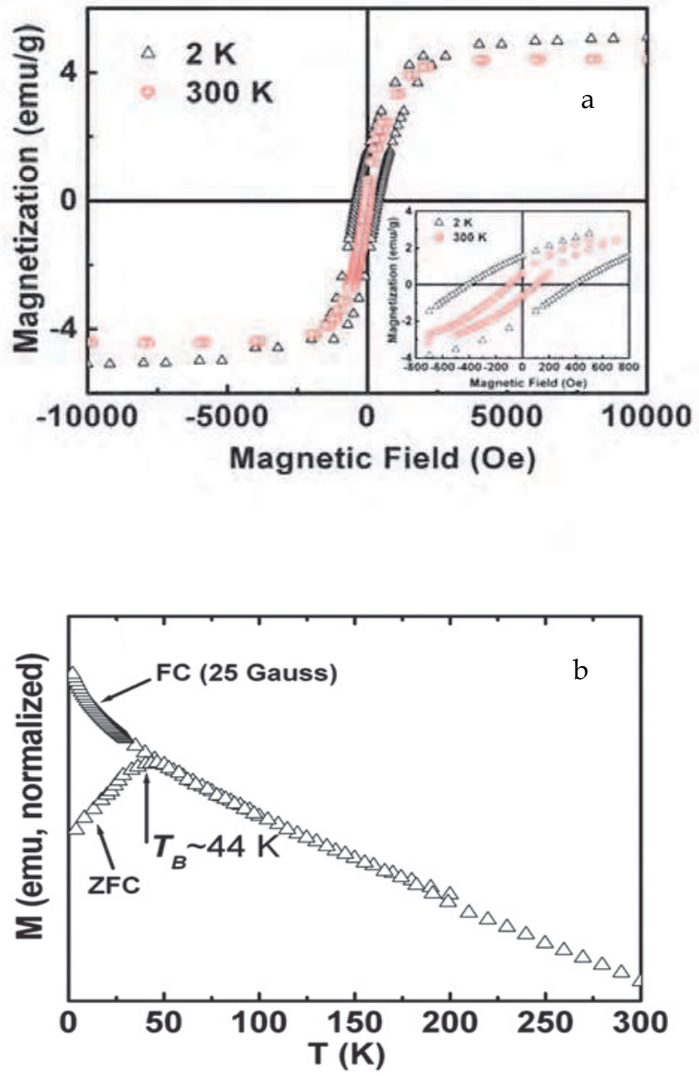

Fig. 13. (a) Magnetization vs. applied magnetic field for nickel nanoparticles deposited VCNTs at 2 K and 300 K. The ferromagnetic behaviour of the sample is apparent from the hysteresis (b) Temperature dependence of ZFC and FC measurements under the applied magnetic field of 25 Gauss for nickel nanoparticle deposited VCNTs.

T/K	M_s/emu g^{-1}	H_c/Oe	M_r/emu g^{-1}
2	5.3	395	1.6
300	4.4	115	0.6

Table 1. M_s, H_c, M_r for Ni nanoparticle deposited VCNTs at 2 K and 300 K.

Figure 14 shows the simplest schematic configuration of the VCNT sample with a STM tip. The nickel substrate act as a source that can generate a current of spin polarised electrons, VCNTs act as a spacer that can transport spin polarised current and the nickel nanoparticle deposit act as a sensor that can detect the spin polarised current. The STM tip acts as contact to the top electrode and the Au to the bottom electrode. The magnetisation of the source defines the spin direction of the charge carriers injected into the CNTs and the nickel coating serves as a spin detector. Upon reversing the magnetisation direction of one of these electrodes, the spin polarisation of the charge carriers arriving at the detector electrode will be changed, giving rise to a change of the device resistivity, i.e., a magnetoresistance.

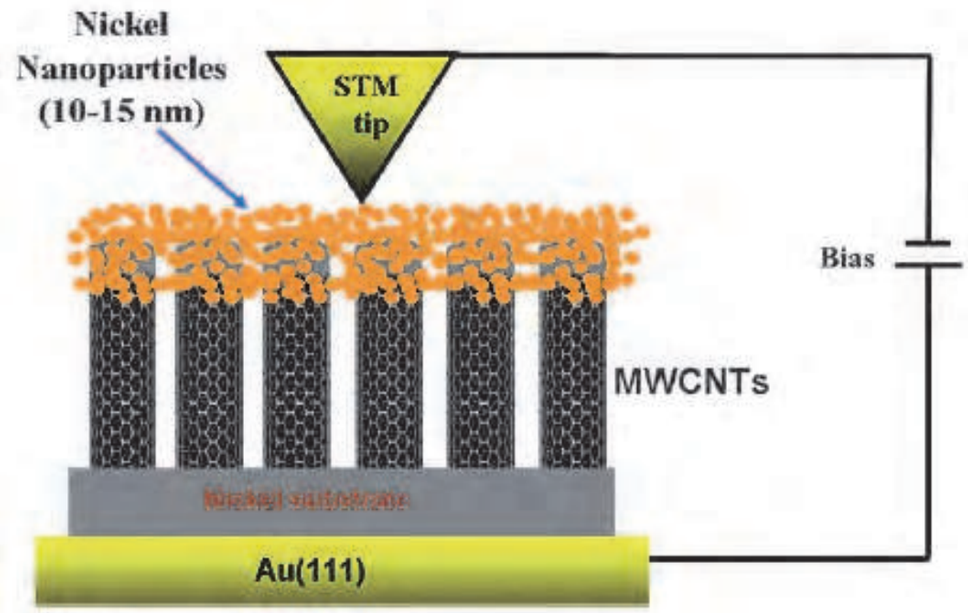

Fig. 14. Schematic diagram of spintronic devices.

Figure 15a shows the current-bias voltage (I-V_b) curves of the sample at H = 0 T and H = 2 T at 300 K. The Coulomb blockade region is observed between -1 V to 1 V and a stepwise increment of the current (CS) is observed beyond the CB region. The (I-V_b) curves exhibit similar features at zero and applied magnetic field (parallel and antiparallel configuration). The similarity in (I-V_b) at zero and applied field is reported in literature. The magnified portion of the green dotted square in the (I-V_b) curves is shown in Figure 15b. A clear CS is apparent in Figure 15b. The dI/dV *vs.* V_b plot (see Figure 15c) exhibits clear peaks in a periodic pattern beyond CB. The dI/dV *vs.* V_b plot in the range (-1.9 to -1 V_b) showing clear periodic pattern is illustrated in the inset of Figure 15c. The bias voltage (V_b) dependence of MR derived from the normalised I-V_b curves shown in Figure 15d. The oscillation of MR as a function of bias voltage is observed.

The ~ null current in the CB region and the CS beyond CB region are clear indications of the SET phenomena. The SET phenomena and the associated MR occur only if the transport of electrons from one electrode to another is inhibited due to the extremely high electrostatic energy $e^2/2C$ (e = charge of electron and C is the capacitance) of a single electron compared to the thermal energy k_BT. When the bias voltage increases and exceeds the threshold $V^{th} = e/2C$, the current starts to increase. If the resistance of two junctions are similar (R1≈ R2), the current increases smoothly with bias voltage. A fluctuation in current is expected if there is difference between the resistances of two junctions. Interestingly, if the difference between the two junction resistances is very large (R1»R2 or R1«R2), the current increases stepwise (CS) with bias voltage depending on the number of electrons accumulated on the spacer. In that case, the tunnelling process in a current-biased junction is no longer random, but becomes more or less coherent (single electron tunnelling), at a frequency $\nu = I/e$. As a result the voltage across the junction will oscillate with the same frequency, and could in principle be used to define a quantum standard for the current.

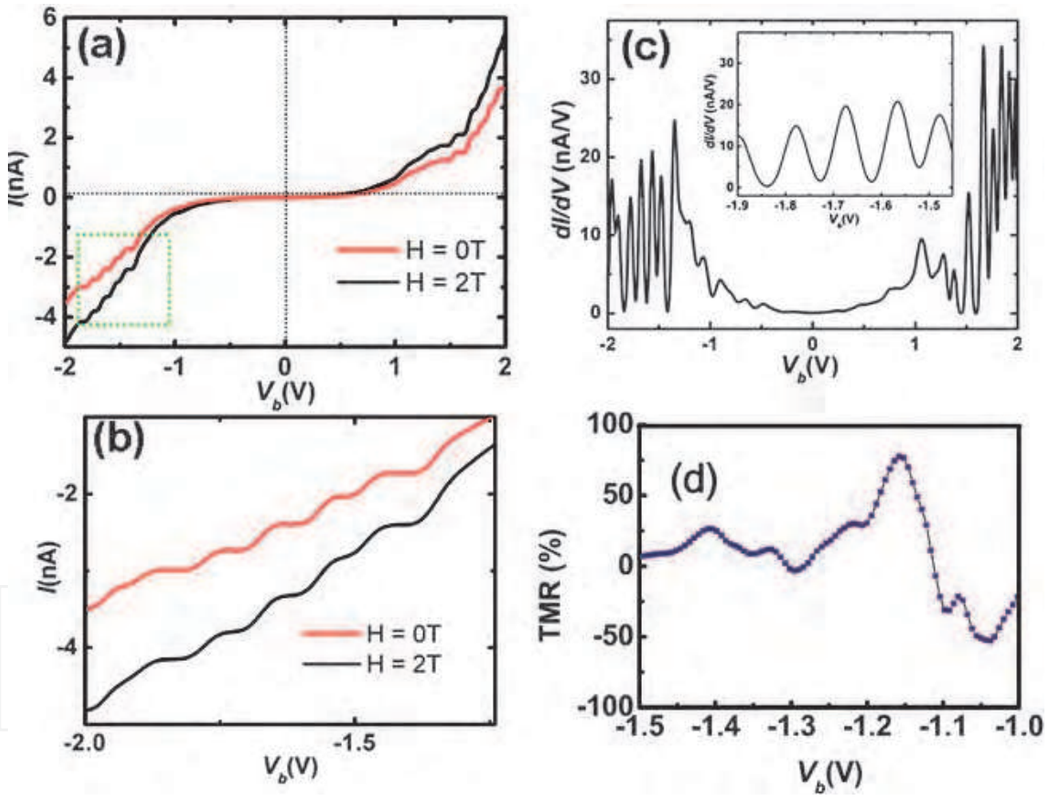

Fig. 15. (a) I–V_b curves of the sample at H = 0 and H =2 T at 300 K, (b) themagnification of the I- V_b (c) the dI/ dV vs. Vb plot of the sample at H= 0 T. (d) The MR% calculated from I–V_b curves. The inset of (c) shows the I–Vb curve in the range -1.9 to -1 Vb.

The calculation of capacitance C is also crucial in determining the TMR effect. We have calculated the capacitance *C* from the period of *dI/dV* curve. The peaks show a periodic pattern with a period of ΔV = 102.0 ±1.8mV. Assuming ΔV = *e*/C, the capacitance is calculated as 1. 5705 × 10^{-18} F. Our result is in agreement with the work of A. B Mantel *et al.*[49] who has studied the spin injection in a single cobalt nanoparticle tunnel junction and they

obtained C value as 1.14 10^{-18} F. The C value calculated by us is consistent with the ferromagnetic nanoparticle tunnel junctions which confirm that the MR effect is due to the spin injection from nickel electrode into the non ferromagnetic CNT and spin detection by the nickel nanoparticle. The MR of the sample was also confirmed by low field measurements (Figure 16). The low field measurements were performed from 100 to 100 Oe and back to 100 Oe. The resistance peak appears as the field moves through zero and it shows a change of resistance from the parallel to antiparallel alignment of the magnetizations.

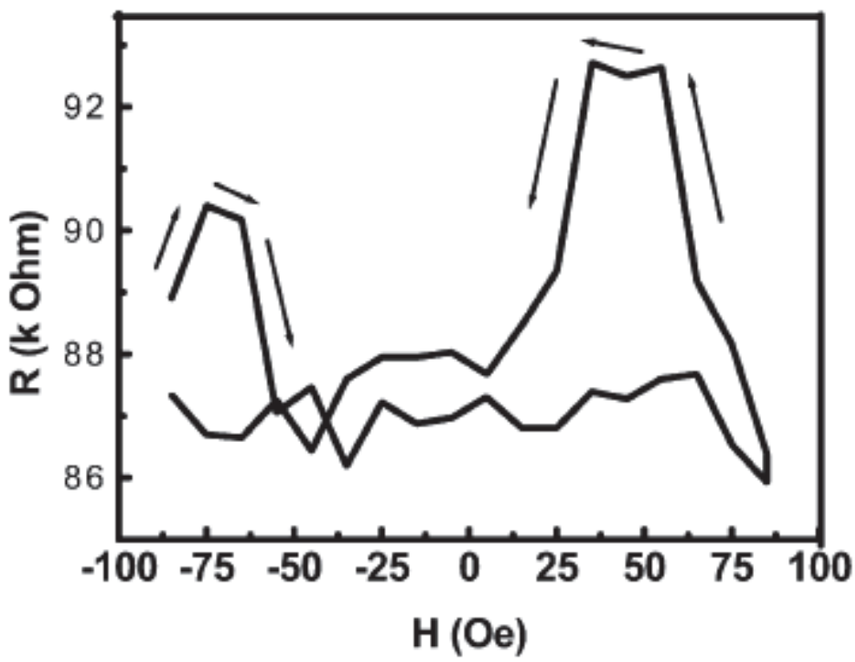

Fig. 16. Schematic of spintronic device showing vertically aligned carbon nanotubes (VCNT) deposited with nickel nanoparticles.

7. Conclusion

The development of room temperature spintronic devices is very motivating for future digital world. Spintronic devices can lead to advances in microelectronics creating faster and high capacity data storage-devices with less power consumption. The spin of the electrons can easily be manipulated in MTJ structures achieving novel phenomena of TMR and SET. However, bringing new or improved MTJs to market requires theoretical modeling and rapid assessment of the effect of enhanced material properties. Carbon nanotubes (CNTs) are ideal spin transporters due to their unique electronic properties.

8. References

[1] Y. Oshima, T.Takenobu, K. Yanagi, Y. Miyata, H. Kataura, K. Hata, Y. Iwasa, and H. Nojiri, Phys. Rev.Lett. 104, 016803 (2010).
[2] B.W. Alphenaar, K. Tsukagoshi, and M. Wagner, Physica E 10, 499 (2001).

[3] S. L.-Mei, G.Wei, C. S.-Xun, and Z. J.-Cang, Chin. Phys. Lett. 9, 3397 (2008).
[4] S.Roche, and R.Saito, Phys. Rev.Lett. 87, 246803 (2001).
[5] X. Hoffer, C. Klinke, J.-M. Bonard, L. Gravier, and J.-E.Wegrowe, Europhys. Lett. 67, 103 (2004).
[6] G. T. Kim, E. S. Choi, D. C. Kim, D. S. Suh, Y. W. Park, K. Liu, G. Duesberg, and S. Roth, Phys. Rev. B 58, 16064 (1998).
[7] F. A. Zwanenburg, D. W. van der Mast, H. B. Heersche, E. P. A. M. Bakkers, and L. P. Kouwenhoven, Nano Lett. 9, 2704 (2009).
[8] S.Krompiewskia, Acta Physica Polonica A, Proceedings of the European Conference Physics of Magnetism, (2008) June 24-27, Poznan, Poland.
[9] A. Bachtold, C. Strunk, J.-P. Salvetat, J.-M.Bonard, L. Forro, T. Nussbaumer, and C. Schonenberger, Nature, 397, 673 (1999).
[10] A. Bachtold, M. Henny, C. Terrier, C. Strunk, C. Schönenberger, J.-P. Salvetat, J.-M. Bonard, and L. Forró, Appl. Phys. Lett.73, 274 (1998).
[11] P. Baláž, Editor *Mechanochemistry in nanoscience and minerals engineering*, Springer, Berlin Heidelberg (2008).
[12] G. Baumgartner, M. Carrard, L. Zuppiroli, W. Bacsa, Walt A. de Heer, and L. Forró, Phys. Rev. B 55, 6704 (1997).
[13] X. Lou, C. Adelmann, S A.Crooker, E S. Garlid, J. Zhang, K. S.M. Reddy, S. D. Flexner, C. J. Palmstrøm, and P. A. Crowell, Nat. Phys. 3, 197 (2007).
[14] B. Zhao, I. Mönch, H. Vinzelberg, T. Mühl, and C. M. Schneider, Appl. Phys. Lett. 80, 3144 (2002).
[15] R.P. Hunt, IEEE Trans. Mag. 7, 150, (1971).
[16] M. N. Baibich, J. M. Broto, A. Fert, F. N. V. Dau, F. Petroff, P. Etienne, G. Creuzet, A. Friederich, and J. Chazelas, Phys. Rev. Lett. 61, 2472 (1988).
[17] H. Sato, P.A. Schroeder, J. Slaughter, W.P. P. Jr., and W. A.-Razzaq, Superlatt. Microstruct. 4, 45 (1988).
[18] T. Miyazaki, and N. Tezuka, J. Magn. Magn. Mater.139, 231 (1995).
[19] Y. M. Lee, J. Hayakawa, S. Ikeda, F. Matsukura, and H. Ohno, Appl. Phys. Lett. 90, 212507 (2007).
[20] Y. M. Lee, J. Hayakawa, S. Ikeda, F. Matsukura, and H. Ohno, Appl. Phys. Lett. 89, 042506 (2006).
[21] M. Julliere, Phys. Lett. 54 225 (1975).
[22] K. Yakushiji, F. Ernult, H. Imamura, K. Yamane, S. Mitani, K. Takanashi, S. Takahashi, S. Maekawa, and H. Fujimori, Nat. Mater. 4, 57 (2005).
[23] J. Mathon and A. Umerski, Phys. Rev. B 63, 220403 (2001).
[24] G. Baumgartner, M. Carrard, L. Zuppiroli, W. Bacsa, Walt A. de Heer, and L. Forró, Phys. Rev. B 55, 6704 (1997).
[25] R. Fiederling, M. Keim, G. Reuscher, W. Ossau, G. Schmidt, A. Waag, and L. W. Molenkamp, Nature (London) 402, 787 (1999).
[26] B. Zhao, I. Mönch, H. Vinzelberg, T. Mühl, and C. M. Schneider, Appl. Phys. Lett. 80, 3144 (2002).
[27] J. Z. Cai, L. Lu1,W. J. Kong, H. W. Zhu, C. Zhang, B. Q. Wei, D. H. Wu, and F. Liu, Phys. Rev. Lett. 97, 026402 (2006).
[28] S. Krompiewski, R. Gutie´rrez, and G. Cuniberti, Phys. Rev. B 69,155423 (2004).
[29] C. Strunk, Science 306, 63 (2004).
[30] X. Hoffer, Ch. Klinke, J.-M. Bonard, L. Gravier, and J.-E. Wegrowe, Europhys. Lett. 67, 103 (2004).

[31] A. N. Chantis, K. D. Belashchenko, E. Y. Tsymbal, and M. V. Schilfgaarde, Phys. Rev. Lett. 98, 046601 (2007).
[32] J. Velev, K. D. Belashchenko, S. S. Jaswal, and E. Y. Tsymbal, Appl. Phys. Lett. 90, 072502 (2007). "
[33] J. Velev, K. D. Belashchenko, D. Stewart, M. van Schilfgaarde, S. S. Jaswal, and E. Y. Tsymbal, Phys. Rev. Lett. 95, 216601 (2005).
[34] K. D. Belashchenko, J. Velev, and E. Y. Tsymbal, Phys. Rev. B 72, R140404 (2005).
[35] K. D. Belashchenko, E. Y. Tsymbal, I. I. Oleinik, and M. V. Schilfgaarde, Phys. Rev. B 71, 224422 (2005).
[36] K. D. Belashchenko, E. Y. Tsymbal, M. V. Schilfgaarde, D. Stewart, I. I. Oleinik, and S. S. Jaswal, Phys. Rev. B 69, 174408 (2004).
[37] F. Sols, F. Guinea, and A. H. CastroNeto, Phys. Rev. Lett. 99, 166803 (2007).
[38] M. Bratkovsky, Appl. Phys. Lett. 72, 2334 (1998).
[39] J. Zhang and R. M. White, J. Appl. Phys. 83, 6512 (1998).
[40] P.P. Dholabhai, R. Atta-Fynn, and A.K. Ray, Eur. Phys. J. B 61, 261 (2008).
[41] S. Yuasa, J. Phys. Soc. Jpn. 77,031001 (2008).
[42] E. Y. Tsymbal, O. N. Mryasov, and P. R. LeClair, J. Phys.: Condens. Matter 15, R109 (2003).
[43] C. Tiusan, F. Greullet, M. Hehn, F. Montaigne, S. Andrieu and A. Schuhl, J. Phys.: Condens. Matter 19,165201(2007).
[44] S. Ikeda, J. Hayakawa, Y. M. Lee, T. Tanikawa, F. Matsukura, and H. Ohno, J. Appl. Phys. 99, 08A907 (2006).
[45] C. Park, J.-G. Zhu, Y. Peng, D.E. Laughlin, and R. M. White, IEEE Trans. Magn. 40, 182 (2004).
[46] N. Tezuka, N. Ikeda, F. Mitsuhashi, and S. Sugimoto, Appl. Phys. Lett. 94, 162504 (2009).
[47] M. T. Johnson, P. J. H. Bloemen, F. J. A. den Broeder and J. J. de Vries,Rep. Prog. Phys. 59 1409 (1996).
[48] S. Yuasa, Y. Suzuki, T. Katayama, and K. Ando, Appl. Phys. Lett. 87, 242503 (2005).
[49] J. Hayakawa, Y. M. Lee, S. Ikeda, F. Matsukura, and H. Ohno, Appl. Phys. Lett. 89, 232510 (2006).
[50] M. G. Wang, C. Ni, A. Rumaiz, Y. Wang, X. Fan, T. Moriyama, R. Cao, Q. Y. Wen, H. W. Zhang, and J. Q. Xiao, Appl. Phys. Lett. 92, 152501 (2008).
[51] S. Ikeda, K. Miura, H. Yamamoto, K. Mizunuma, H. D. Gan, M. Endo, S. Kanai, J. Hayakawa, F. Matsukur and H. Ohno, Nat. Mat. 9, 721(2010).
[52] J. S. Moodera, L. R. Kinder, T. M. Wong, and R. Meservey, Phys. Rev. Lett. 74, 3273 (1995).
[53] S.S.P. Parkin, K.P. Roche, M.G. Samant, P.M. Rice, R.B. Beyers, R.E. Scheuerlein, E.J. O'Sullivan, S.L. Brown, J. Bucchigano, D.W. Abraham, Y. Lu, M. Rooks, P.L. Trouilloud, R.A. Wanner, and W.J. Gallagher, J. Appl. Phys. 85, 5828 (1999).
[54] R. Wiesendanger, Editor *Scanning Probe Microscopy and Spectroscopy*, New York: Cambridge University Press, 1994.
[55] L. E. Hueso, J. M. Pruneda, V. Ferrari, G. Burnell, J. P. V. -Herrera, B. D. Simons, P. B. Littlewood, E. Artacho, A. Fert, and N. D. Mathur, Nature 445, 410 (2007).
[56] R. S. Liu, H. Pettersson, L. Michalk, C. M. Canali, and L. Samuelson, Nano Lett. 7, 81 (2007).
[57] H. B. Peng and J. A. Golovchenko, Appl. Phys. Lett. 84, 5428 (2004).
[58] E. Titus, M. K. Singh, G. Cabral,V.Paserin, P. R. Babu, W.J. Blau, J. Ventura, J. P. Araujo, and J. Gracio, J. Mater. Chem. 19, 7216 (2009).
[59] T. Niizeki, H. Kubota, Y. Ando, and T. Miyazaki, J. Magn.Magn. Mater. 272, 1947 (2004
[60] N. Tombros, S. J. van der Molen, and B. J. van Wees, Phys. Rev. B 73, 233403 (2006).
[61] C. Chappert, Albert Fert, and F. N. V. Dau, Nat. Mat.6,813 (2007).
[62] S. Sanvito, Nat. Nanotechnol. 2, 204 (2007).

[63] I. Appelbaum, B. Huang, and D. J. Monsma, Nature 447, 295 (2007).
[64] E. Y. Tsymbal, K. D. Belashchenko, J. Velev, S. S. Jaswal, M. V. Schilfgaarde, I. I. Oleynik, and D. A. Stewart, Prog. Mater. Science 52, 401 (2007).
[65] A. N. Chantis, K. D. Belashchenko, D. L. Smith, E. Y. Tsymbal, M. V. Schilfgaarde, and R. C. Albers, Phys. Rev. Lett. 99, 196603 (2007).
[66] L. Berger, J. Appl. Phys. 49, 2156 (1978).
[67] E. Y. Tsymbal, K. D. Belashchenko, J. Velev, S. S. Jaswal, M. V. Schilfgaarde, I. I. Oleynik, and D. A. Stewart, Prog. Mater. Science 52, 401 (2007).
[68] A. N. Chantis, K. D. Belashchenko, D. L. Smith, E. Y. Tsymbal, M. V. Schilfgaarde, and R. C. Albers, Phys. Rev. Lett. 99, 196603 (2007).
[69] J. D. Burton, R. F. Sabirianov, J. P. Velev, O. N. Mryasov, and E. Y. Tsymbal, Phys. Rev. B 76, 144430 (2007).
[70] H. Suzuura, and T.Ando, Physica E 6, 864 (2000).
[71] J.-G. Zhu and C. Park, Mater. Today 9, 36 (2006).
[72] R. Arras, L. Calmels, and B. Warot-Fonrose, IEEE Trans. Magn.46, 1730 (2010).
[73] N. M. Caffrey, T. Archer, I. Rungger, and S. Sanvito, Phys. Rev. B. 83, 125409 (2011).
[74] M. Stilling, K. Stokbro, and K. Flensberg, J. Comp. Aided Mater. Des. 14, 141 (2007).
[75] Y. Ke, K. Xia, and H. Guo, Phys.Rev. Lett. 100, 166805 (2008).
[76] D. Waldron, L. Liu and H. Guo, Nanotechnology 18, 424026 (2007).
[77] N. L. Chung, M. B. A. Jalil, and S. G. Tan, J. Phys. D: Appl. Phys. 42, 195502 (2009).
[78] R. Landauer, IBM J. Res. Dev. 1, 233 (1957).
[79] K.S. Novoselov, A.K. Geim, S.V. Morozov, D. Jiang, Y. Zhang, S.V. Dubonos, I.V. Grigorieva, and A.A. Firsov, Science 306, 666 (2004).
[80] Y. Zhang, Y.-W. Tan, H.L. Stormer, and P. Kim, Nature 438, 201 (2005).
[81] A.K. Geim and K.S. Novoselov, Nature Mater. 6, 183 (2007).
[82] K. I. Bolotin, K. J. Sikes, J. Hone, H. L. Stormer, and P. Kim, Phys. Rev. Lett. 101, 096802 (2008).
[83] M. Maiti and K. Sengupta, Phys. Rev. B 76, 054513 (2007).
[84] S. Yuasa, T. Nagahama and Y. Suzuki, Science 297, 234 (2002).
[85] O.V. Yazyev and L. Helm, Phys. Rev. B 75, 125408 (2007).
[86] C. Bai and X. Zhang, Phys. Lett. A 372, 275 (2008).
[87] K.S. Novoselov, A.K. Geim, S.V. Morozov, D. Jiang, M.I. Katsnelson, I.V. Grigorieva, S.V. Dubonos, and A.A. Firsov, Nature 438, 197 (2005).
[88] E. W. Hill, A. K. Geim, K. Novoselov, F. Schedin, and P. Blake, IEEE Trans. Magn. 42, 2694 (2006).
[89] C. L. Kane and E. J. Mele, Phys. Rev. Lett. 95, 226801 (2005).
[90] F. J. Jedema, A. T. Filip, and B. J. van Wees, Nature 410, 345 (2001).
[91] S. Sahoo, T. Kontos, J. Furer, C. Hoffmann, M. Gräber, and C. Schönenberger, Nat. Phys. 1, 99 (2005).
[92] L. Gammaitoni, P. Hänggi, P. Jung, and F. Marchesoni, Rev. Mod. Phys. 70, 223 (1998).
[93] A. De Martino and R. Egger, J. Phys.: Condens. Matter 17, 5523 (2005).
[94] S. Garzon, I. Zutic, and R. A. Webb, Phys. Rev. Lett. 94, 176601 (2005).
[94] M. Bockrath, D. H. Cobden, P. L. McEuen, N. G. Chopra, A. Zettl, A. Thess, and R. E. Smalley, Science 275, 1922 (1997).
[95] N. Tombros, S. J. van der Molen, and B. J. van Wees, Phys. Rev. B 73, 233403 (2006).
[96] B.-C. Min, K. Motohashi, C. Lodder, and R. Jansen, Nat. Mater. 5, 817 (2006).
[97] L. I. Glazman and K. A. Matveev, JETP Lett. 48, 445 (1988).
[98] D. J. Monsma and S. S. P. Parkin, Appl. Phys. Lett. 77, 720 (2000).
[99] K. P. Kamper, W. Schmitt, G. Guntherodt, R. J. Gambino, and R. Ruf, Phys. Rev. Lett. 59, 2788 (1987).

[100] W. A. Hofer, A. S. Foster, and A. L. Shluger, Rev. Mod. Phys. 75, 1287 (2003).
[101] D. J. Monsma and S. S. P. Parkin, Appl. Phys. Lett. 77, 720 (2000).
[102] W. Liang, M. Bockrath, and H. Park, Phys. Rev. Lett. 88, 126801 (2002).
[103] K. Tsukagoshi, B. W. Alphenaar, and H. Ago, Nature 401, 572 (1999).
[104] J.M. Bonard, F. Maier, T. Stockli, A. Chatelain, W. A. Heer, J.P. Salvetat, and L. Forro, Ultramicroscopy 73 ,7 (1998).
[105] L. Dai, A. Patil, X.Y. Gong, Z.X. Guo, L.Q. Liu, Y. Liu, D.B. Zhu, Chem. Phys. Lett. 4 ,1150 (2003).
[106] W.I. Milne, K.B.K. Teo, E. Minoux, O. Groening, L. Gangloff, L. Hudanski, J.P. Schnell, D. Dieumegard, F. Peauger, I.Y.Y. Bu, M.S.Bell, and P. Legagneux, J.Vacuum Sci. Technol. 24, 345 (2006).
[107] M. Chhowalla, C. Ducati, N.L. Rupesingh, K.B.K. Teo, and G.A.J. Amaratunga, Appl.Phys. Lett. 79 , 2079 (2001).
[108] K.B.K. Teo, M. Chhowalla, G.A.J. Amaratunga, W.I. Milne, G. Pirio, P. Legagneux, F. Wyczisk, D. Pribat, and D.G.Hasko, Appl. Phys. Lett. 80 , 2011 (2002).
[109] J.M. Bonard, F. Maier, T. Stockli, A. Chatelain, W.A. de Heer, J.P. Salvetat, and L.Forro, Ultramicroscopy 73 , 7 (1998).
[110] M.S. Kabir, R.E. Morjan, O.A. Nerushev, P. Lundgren, S. Bengtsson, P. Enoksoni, and E.E.B. Campbell, Nanotechnology 16, 458 (2005).
[111] Z.F. Ren, Z.P. Huang, and J.W.Xu, Science 282 , 1105 (1998).
[112] C. Taschner, F. Pacal, A. Leonhardt, P. Spatenka, K. Bartsch, and A.Graff, Surface Coatings Technol. 81, 174 (2003).
[113] G. Cabral, E.Titus , D. S. Misra, and J.Gracio, J Nanosci Nanotechnol. 8, 4029 (2008).
[114] M. Wienecke, C. Mihaela, K. Deistung, P. Fedtke, and E.Borchartd, Carbon 44 , 718 (2006).
[115] C. Bower, O .Zhou, W. Zhu, D.J. Werder, and S .Jin, Appl. Phys. Lett.77, 2767 (2000).
[116] J.G. Wen, Z.P. Huang, D.Z. Wang, J.H. Chen, S.X. Yang, and Z.F. Ren, J.Mater Res. 16, 3246 (2001).
[117] A.M. Rao, A. Jorio, M.A. Pimenta, M.S.S. Dantas, R. Saito, G. Dresselhaus, M.S. Dresselhaus, Phys. Rev. Lett. 84 , 1820 (2000).
[118] A. Jensen, J. R. Hauptmann, J. Nygard, and P. E. Lindelof, Phys. Rev. B, 72, 035419 (2005).
[119] Z. H. Xiong, D. Wu, Z. V. Vardeny, and J. Shi, Nature 427, 821 (2004).
[120] H. Shimada, K. Ono, and Y. Ootuka, J. Phys. Soc. Jpn. 67, 1359 (1998).
[121] P. L. McEuen, M. Fuhrer, and H. Park, IEEE Trans. Nanotechnol. 1,78 (2002).
[122] J. M. de Teresa, A. Barthélémy, A. Fert, J. P. Contour, F. Montaigne, and P. Seneor, Science, 286,507 (1999).
[123] S. Yuasa, T. Nagahama, A. Fukushima, Y. Suzuki, and K. Ando, Nat.Matr.3, 868 (2004).
[124] E. Titus, M.K. Singh, Gil Cabral, V. Paserin, Ramesh Babu P, W.J. Blau, and J. Gracio, J. Nanosci. Nanotechnol. 10, 2606 (2010).
[125] I. Bergenti, A. Deriu, E. Bosco, M. Baricco, E. Angeli, D. Bisero, A. Da Re, F. Ronconi, F. Spizzo, and P. Vavassori, J. Magn. Magn. Mater. 272–276, 1554 (2004).
[126] S. Kenane, J. Voiron, N. Benbrahim, E. Chainet, and F. Robaut, J. Magn. Magn. Mater. 297, 99 (2006).
[127] Y. Li, T. Kaneko, T. Ogawa, M. Takahashi, and R. Hatakeyamma, Chem. Commun. 254, (2007).
[128] F. C. Fonseca, G. F. Goya, R. F. Jardim, R. Muccillo, N. L. Carre~no, E. Longo, and E. R. Leite, Phys. Rev. B 66, 104406 (2002).
[129] S. Linderoth, L. Balcells, A. Labarta, J. Tejada, P. V. Hendriksen, and S. A. Sethi, J. Magn. Magn. Mater. 124, 269 (1993).

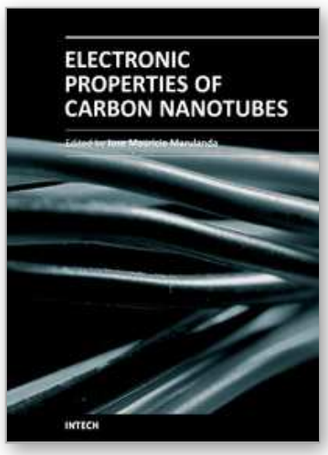

Electronic Properties of Carbon Nanotubes

Edited by Prof. Jose Mauricio Marulanda

ISBN 978-953-307-499-3
Hard cover, 680 pages
Publisher InTech
Published online 27, July, 2011
Published in print edition July, 2011

Carbon nanotubes (CNTs), discovered in 1991, have been a subject of intensive research for a wide range of applications. These one-dimensional (1D) graphene sheets rolled into a tubular form have been the target of many researchers around the world. This book concentrates on the semiconductor physics of carbon nanotubes, it brings unique insight into the phenomena encountered in the electronic structure when operating with carbon nanotubes. This book also presents to reader useful information on the fabrication and applications of these outstanding materials. The main objective of this book is to give in-depth understanding of the physics and electronic structure of carbon nanotubes. Readers of this book should have a strong background on physical electronics and semiconductor device physics. This book first discusses fabrication techniques followed by an analysis on the physical properties of carbon nanotubes, including density of states and electronic structures. Ultimately, the book pursues a significant amount of work in the industry applications of carbon nanotubes.

How to reference

In order to correctly reference this scholarly work, feel free to copy and paste the following:

Elby Titus, Rahul Krishna, José Grácio, Manoj Singh, Antonio Luis Ferreira and Ricardo G Dias (2011). Carbon Nanotube Based Magnetic Tunnel Junctions (MTJs) for Spintronics Application, Electronic Properties of Carbon Nanotubes, Prof. Jose Mauricio Marulanda (Ed.), ISBN: 978-953-307-499-3, InTech, Available from: http://www.intechopen.com/books/electronic-properties-of-carbon-nanotubes/carbon-nanotube-based-magnetic-tunnel-junctions-mtjs-for-spintronics-application

INTECH
open science | open minds

InTech Europe
University Campus STeP Ri
Slavka Krautzeka 83/A
51000 Rijeka, Croatia
Phone: +385 (51) 770 447
Fax: +385 (51) 686 166
www.intechopen.com

InTech China
Unit 405, Office Block, Hotel Equatorial Shanghai
No.65, Yan An Road (West), Shanghai, 200040, China
中国上海市延安西路65号上海国际贵都大饭店办公楼405单元
Phone: +86-21-62489820
Fax: +86-21-62489821

IntechOpen